ELSEVIER

Diamond and Related Materials 11 (2002) 969–975

DIAMOND AND RELATED MATERIALS

www.elsevier.com/locate/diamond

Growth mechanism of amorphous hydrogenated carbon

A. von Keudell*, M. Meier, C. Hopf

Centre for Interdisciplinary Plasma Science, Max-Planck-Institut für Plasmaphysik, EURATOM Association, Boltzmannstr. 2, 85748 Garching, Germany

Abstract

Amorphous hydrogenated carbon (a-C:H) films offer a wide range of applications due to their extraordinary material properties like high hardness, chemical inertness and infrared transparency. The films are usually deposited in low temperature plasmas from a hydrocarbon precursor gas, which is dissociated and ionized in the plasma and radicals and ions impinging onto the surface leading to film growth. Final stoichiometry and material properties depend strongly on composition, fluxes and energy of the film forming species. The underlying growth mechanisms are investigated by means of quantified particle beam experiments employing radical sources for atomic hydrogen (H) and methyl (CH_3) radicals as well as an argon ion beam. The interaction of these species with amorphous hydrogenated carbon films is investigated in real time by ellipsometry and infrared spectroscopy. The formation of hydrocarbon films from beams of CH_3, H and Ar^+ is considered a model system for growth of amorphous hydrogenated carbon films in low temperature plasmas from a hydrocarbon precursor gas. The growing film surface can be separated in a chemistry-dominated growth zone with a thickness of 2 nm on top of an ion-dominated growth zone. In the chemistry-dominated growth zone incident atomic hydrogen governs the surface activation as well as film stoichiometry. In the ion-dominated growth zone, especially hydrogen ions, displace bonded hydrogen in the film. Displaced hydrogen recombine and form H_2 molecules, which desorb. This leads to a low hydrogen content of the films.

Keywords: Amorphous hydrogenated carbon; Growth; Plasma

1. Introduction

Amorphous hydrogenated carbon films (a-C:H) are used in many applications due to their extraordinary material properties like high hardness, infrared transparency or chemical inertness [1–4]. Hydrocarbon films have a typical hydrogen atom concentration ranging from 30% to above 50%. The hydrogen content depends strongly on the kinetic energy of the impinging ions during plasma-deposition. Films with a hydrogen atom concentration of $\sim$50% are formed at low ion energies with almost all carbon atoms being sp^3-hybridized. Due to the soft structure, the films are named polymer-like amorphous carbon films. At higher ion energies $>$50 eV, the hydrogen atom concentration decreases to 30% and $\sim$60% of the carbon atoms in these films are sp^2-hybridized. The resulting film structure is dense and hard, which led to the expression diamond-like amorphous carbon films. The correlation between kinetic energy of the incident ions impinging and film composition is explained by the preferential displacement of bonded hydrogen in a collision cascade: penetrating ions displace predominantly bonded hydrogen due to the smaller threshold energy for displacement of hydrogen (2.5 eV) compared to that of carbon (25 eV) [5]. The displaced hydrogen atoms can recombine with a lattice defect or form H_2 molecules by recombination with another displaced H atom. These H_2 molecules are either trapped in internal voids or diffuse to the surface and desorb [6]. Consequently, the hydrogen content decreases with increasing ion energy.

Ion-induced effects during thin film deposition are often described by computer simulations based on the binary collision approximation (BCA) [7]. Such models were successfully applied to the ion beam deposition of amorphous carbon films like tetrahedral-amorphous carbon (ta-C) [8,9]. In the case of a-C:H films, however, the plasma growth process is influenced by the presence of thermal hydrocarbon radicals and atomic hydrogen. These heterogeneous surface processes can lead to very

*Corresponding author. Tel.: +49-89-3299-1631; fax: +49-89-3299-1149.

E-mail address: von_keudell@ipp.mpg.de (A. von Keudell).

0925-9635/02/$ - see front matter
PII: S0925-9635(01)00553-2

different results for growth rates and film composition in comparison to the ion based deposition systems.

Many different radicals contribute to the plasma composition of a low-temperature hydrocarbon plasma. This complexity is caused by gas phase reactions among the primary dissociation products of the feed gas. In a CH_4 electron cyclotron resonance (ECR) discharge from methane at a pressure of 1 Pa, ionic species up to $C_{14}H_y^+$ and neutral species up to C_3H_y were observed by mass spectrometry [10]. The larger positive ions are most probably produced by ion–neutral reactions in the bulk plasma due to the larger cross-sections for ion–neutral collisions compared to neutral–neutral collisions. The hydrocarbon radical with the largest plasma density in a methane discharge is methyl (CH_3), as identified and quantified by threshold ionization mass spectrometry (TIMS) [11].

The contribution of incident radicals to film formation is characterized by the surface loss probability β, which corresponds to 1 minus the reflection coefficient. The surface loss probability β can be measured in a plasma experiment by two complementary methods: the *decay technique*, which is sensitive to growth precursors with $\beta < 10^{-2}$ and the *cavity technique*, which is sensitive to growth precursors with $\beta > 0.1$. In the *decay technique*, the flux of a specific radical impinging onto a surface is monitored by time-resolved mass spectrometry in the pulse pause of a pulsed discharge. The surface loss probability β is derived from a modelling of the decay of the radical density in the pulse pause. By using this technique, Toyoda et al. [12] measured $\beta(CH_3) < 10^{-3}$ and $\beta(CH_2) \sim 0.025$. Shiratani et al. [13] measured $\beta(CH_3)$ ranging from 10^{-3} to 0.014. Finally, Perrin et al. [14] measured a $\beta(C_2H_5)$ of 0.025. In the *cavity technique* a small cavity is exposed to a low-temperature plasma. The cavity consists of a closed volume with a small opening through which species, emanating from the plasma, enter and undergo multiple surface collisions inside. The film thickness profile (=deposition profile) of the layers formed inside the cavity depends on the surface loss probability β. The absolute value of the surface loss probability β is derived from a comparison of the deposition profile with a Monte Carlo simulation of the transport of species inside the cavity. Hopf et al. [15,16] used the cavity technique to determine the surface loss probabilities of hydrocarbon radicals emanating from various hydrocarbon discharges. They identified three characteristic growth precursors [15,16]: sp^1-hybridized precursors like C_2H have a β of ~0.9, sp^2-hybridized precursors have a β of ~0.35 and sp^3-hybridized precursors have a $\beta < 10^{-2}$.

Besides carbon-carrying radicals, atomic hydrogen (H) is formed from every hydrocarbon precursor gas via dissociation in the discharge. Due to the inefficient pumping of hydrogen in most plasma reactors, atomic hydrogen builds up a rather large density and contributes, therefore, significantly to the impinging radical flux onto a growing film surface. In many experiments it was observed that the a-C:H growth rate in a low-temperature plasma decreases with increasing substrate temperature. This general behavior is caused by a balance between a temperature-independent incorporation of hydrocarbon radicals during film deposition and a temperature-dependent re-etching of the films by atomic hydrogen [17].

To summarize: (i) the surface loss probabilities of various hydrocarbon radicals range from $< 10^{-2}$ for sp^3-hybridized precursor to almost unity for sp^1-hybridized precursors; (ii) the temperature dependence of film formation is caused by the re-etching by atomic hydrogen; (iii) energetic ion bombardment lowers the hydrogen content in the films. This current understanding of a-C:H film growth was deduced from plasma experiments by measuring growth rates vs. process parameters like substrate temperature, bias voltage or plasma power. Such a reasoning, however, can still be misleading since many species interact with the growing film surface simultaneously and a specific conclusion might be ambiguous. One approach to gain a much more detailed insight in growth processes is the use of particle beam experiments. With such experiments, it is possible to isolate specific growth mechanisms and to obtain quantitative data like cross-sections or rate coefficients.

Over recent years, we implemented such a particle beam experiment to study thin film growth processes in methane discharges [18–21]. We restrict ourselves for the design of the particle beam experiments to consider only methyl radicals and atomic hydrogen as the most important radicals. As a third particle beam, we implemented an argon ion beam in our experiment. In this view, we consider the formation of hydrocarbon films from particle beams of H, CH_3 and ions as a model system for film formation in a hydrocarbon low temperature plasma. In this paper we address the question about the influence of the various ion–radical or radical–radical growth synergisms on film formation.

2. Experiment

Surface processes during thin film growth are studied by exposing an amorphous hydrogenated carbon film to a known flux of methyl radicals, atomic hydrogen and argon ions. A schematic sketch of the experimental setup is shown in Fig. 1. The experiment is separated into a preparation chamber, which serves also as load lock for the samples. In the preparation chamber, C:H films are deposited by means of an r.f. discharge from CH_4 at a pressure of 2 Pa and a d.c. self-bias of −300 V. The thickness of the C:H films is ~20–40 nm. The films have an H/C ratio of 0.41 and a density of approximately 1.9 g cm^{-3}, as determined by ion-beam analysis. The film properties are typical of so-called

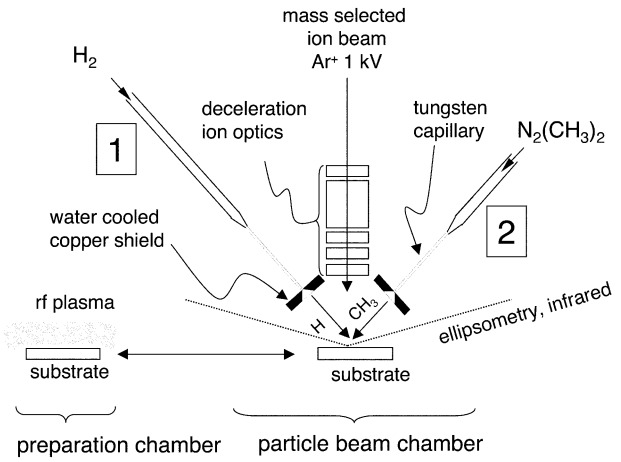

Fig. 1. Sketch of the experimental setup. A-C:H films are deposited from a r.f. discharge from methane in a preparation chamber. The samples are transferred in vacuo in the particle beam chamber equipped with two radical sources for H and CH_3 and a mass and energy selected ion beam.

'hard' carbon films. The samples are transferred from the preparation chamber into the radical beam chamber without breaking the vacuum.

The particle beam chamber is equipped with two radical beam sources for production of H and CH_3. The radicals are produced via thermal dissociation of H_2 or azomethane $N_2(CH_3)_2$ in a heated tungsten capillary. The implementation and the performance of the radical beam sources are described in great detail elsewhere [18,19]. The capillaries of the radical sources are constantly heated in order to maintain thermal equilibrium of the whole setup and the fluxes are switched on and off by switching on and off the gas flow. Without additional external heating of the substrates the sample temperature adjusts under these conditions to 320 K.

A commercial Colutron ion gun is used to produce a mass selected ion beam. Ions are extracted from the ion source and accelerated to 1 kV. After mass separation in a Wien filter, the ions can be decelerated to energies down to 100 V (see Fig. 1). In order to prevent high energy neutrals from charge exchange collisions between the 1 kV ions and background gas, the ion beam is bent by 2° with deflector plates prior its deceleration. The ion current onto the sample is determined by measuring the current between sample holder and ground. Such a simple procedure neglects the contribution of secondary electron emission to the measured current, which limits the accuracy of the current measurement to roughly a factor of 2. A more thorough calibration of the ion current will be implemented soon.

Growth and erosion of hydrocarbon films during exposure to the CH_3 and H beam is monitored by a rotating analyzer ellipsometer to measure the ellipsometric angles Ψ and Δ. The angle of incidence is $\sim 75.8°$ and the optical properties are measured at a wavelength of 632.8 nm. For each data point 50–100 revolutions of the analyzer are averaged followed by the measurement of the background light, yielding a time separation of the data points of 3.38–5.9 s. The accuracy in Ψ is $\delta\Psi = 0.005°$ and in Δ is $\delta\Delta = 0.02°$.

3. Results

3.1. Adsorption of hydrocarbon radicals

A C:H film surface is exposed to the H and CH_3 radical beams. The H flux is 1.4×10^{15} cm^{-2} s^{-1} and the CH_3 flux is 3×10^{14} cm^{-2} s^{-1}. The variation of the CH_3 and H flux during the experiment is shown in Fig. 2b,c, respectively. Fig. 2a shows the resulting growth rate expressed in incorporated carbon atoms per area and time. In the beginning of the experiment only the CH_3 beam is on. From a dedicated CH_3 adsorption experiment [21], the sticking coefficient of methyl alone is measured only to be $s(CH_3) \sim 10^{-4}$. Between 380 s and 6340 s, the H beam is switched on additionally. After a gradual increase in the beginning, the growth rate reaches steady state, corresponding to an effective sticking coefficient of $s(CH_3|H) \sim 10^{-2}$. After switching the H beam off, the growth rate drops sharply. In the following, the H beam is switched on again. Between

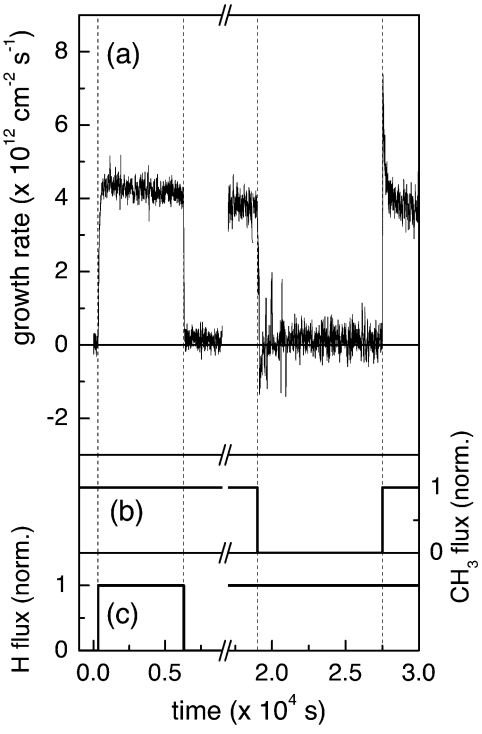

Fig. 2. (a) Variation of the growth rate during the interaction of an a-C:H film with the H and CH_3 radical beam at a substrate temperature of 320 K. (b) Variation of the CH_3 flux normalized to 3×10^{14} cm^{-2} s^{-1}. (c) Variation of the H flux normalized to 1.4×10^{15} cm^{-2} s^{-1}.

19 000 s and 27 500 s the CH_3 beam is switched off and on. In the beginning at $t>19000$ s, a slight etching of the film is observed, which disappears again at $t>$ 20 000 s. In the following, hydrogen chemical erosion occurs only at a very small rate in the range of the experimental errors. At $t=27\,500$ s, the CH_3 beam is switched on and film growth sets in. After a sharp increase in the beginning, the growth rate decreases again and reaches steady state, corresponding to an effective sticking coefficient of $s(CH_3|H)\sim 10^{-2}$. This experiment illustrates that the simultaneous interaction of H and CH_3 with a C:H film surface leads to a significant growth synergism.

This observation is explained as follows: it is assumed that growth occurs due to chemisorption of CH_3 radicals at dangling bonds at the surface. Dangling bonds are created via abstraction of surface-bonded hydrogen by incident H or CH_3. The cross-section for hydrogen abstraction by H is $\sigma_{\text{abstraction,H}}=0.05$ Å^2 and for hydrogen addition to a dangling bond is $\sigma_{\text{addition, H}}=1.3$ Å^2 [22]. Based on the cross-sections for the surface reactions of H, it is possible to determine the cross-sections for the surface reactions of CH_3 from a simple balance equation model [21]: chemisorption of CH_3 at a dangling bond at the surface yields $\sigma_{\text{addition, CH}_3}$ between 2.4 and 5.9 Å^2 and abstraction of surface-bonded hydrogen by methyl radicals yields $\sigma_{\text{abstraction, CH}_3}$ of $\sim 10^{-3}$ Å^2. The fact that $\sigma_{\text{abstraction, H}}$ is much larger than $\sigma_{\text{abstraction, CH}_3}$ becomes apparent as a huge growth synergism between H and CH_3.

In an extended balance equation model [23,24], it is taken into account that CH_3 chemisorption at surface dangling bonds forms in a first step tri-hydride surface groups. These tri-hydride groups can be cross-linked to di- and mono-hydride groups via hydrogen elimination reactions. This hydrogen elimination reactions consists of the sequence of abstraction of surface-bonded hydrogen by incident H followed by dangling-bond recombination. This recombination, however, requires structural changes in the amorphous network, such as bond angle and/or bond length variations. The change of the local carbon network structure has, according to the random covalent network (RCN) theory [25,26], a low activation energy, if the network is *under-constrained*. As a consequence, hydrogen elimination becomes increasingly more difficult if a *fully-constrained* network is approached. This results in a stoichiometric limit of H/C$\sim$1 for the H-induced reduction of the hydrogen content of a-C:H films, in agreement with the RCN theory.

The existence of partly tri-hydride terminated surface is also able to explain the observed dynamic of the film formation process. The slight etching at $t>19\,000$ s in Fig. 2 is caused by the H-induced removal of CH_3 endgroups from the surface. The excess in growth rate for $t>27\,500$ s in Fig. 2 is caused by the re-formation of a partly tri-hydride terminated surface via CH_3 chemisorption. Details of this analysis and the experimental verification of a tri-hydride terminated surface via infrared spectroscopy can be found in Meier and von Keudell [23].

The growth synergism between CH_3 and H implicates that the use of a fixed sticking coefficient for CH_3 is not adequate to model a-C:H growth in low-temperature plasmas. Instead, the absolute value for $s(CH_3)$ depends on the fluxes of other incident species (radicals and ions), which interact simultaneously with the growing film surface. This interrelation also explains the widely differing values for the surface loss probability $\beta(CH_3)$ in the literature [12–14]. In the case of a small contribution of atomic hydrogen to the flux towards the surface in a specific plasma experiment, only small values for $\beta(CH_3)$ are measured. In the case of a very large H contribution, however, much higher values of $\beta(CH_3)$ are obtained.

3.2. Ion-induced effects

The bombardment of the growing film surface with energetic ions is believed to be a key step in layer formation. Within a collision cascade, penetrating ions displace mainly bonded hydrogen in the film. Displaced hydrogen atoms might recombine to form H_2 molecules, which eventually desorb. If a hydrogen atom is displaced at the physical surface a surface dangling bond is formed, which then serves as chemisorption site for incoming radicals. This ion-induced activation of the surface followed by C_xH_y chemisorption has been coined 'ion-stitching' [27]. It is expected that 'ion stitching' has only a weak substrate temperature dependence. The temperature dependence of C:H film growth is dominated by the thermal stability of the surface dangling bonds. The thermally activated relaxation of dangling bonds causes a release of C_xH_y end groups, if the film is hydrogen- and sp^3-rich. Such a film composition, however, is not the stable steady state composition in the case of a significant ion bombardment. As a consequence, the ion bombardment suppresses the chemical etching of the films. This has been directly observed in experiments for the interaction of hydrogen plasmas with C:H films [17].

The ion-induced effects are illustrated by simulations using the computer code TRIM to quantify the amount of displaced hydrogen in a a-C:H film within a collision cascade for a 200-eV C^+ ion and a 200-eV H^+ ion, respectively. The necessary input parameters for displacement thresholds and surface binding energies are taken from Möller [5]. The number of displaced hydrogen atoms per ion and nm in a film with H/C ratio of 0.3:0.7 is shown in Fig. 3. It can be seen that the penetration depth of the C^+ ions is only $\sim$2 nm and a total of approximately five hydrogen atoms are displaced

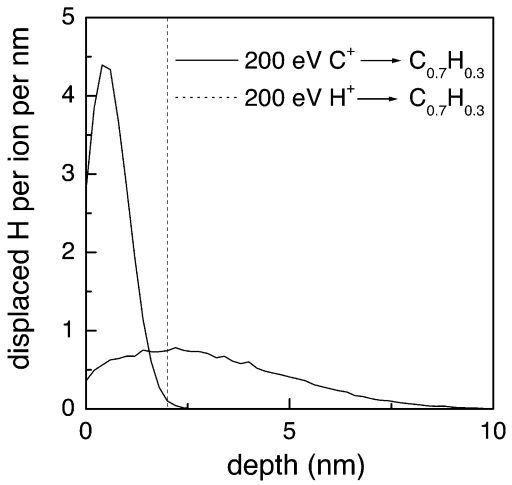

Fig. 3. TRIM calculation for the displacement of bonded hydrogen atoms per nm and ion in a $C_{0.7}H_{03}$ film for incident hydrogen and carbon ions with a kinetic energy of 200 eV. The vertical dotted line indicates the penetration depth of incident thermal hydrogen atoms.

within this range. In the case of hydrogen ions, however, the penetration depth of H^+ ions extends up to 10 nm and a total of approximately four hydrogens are displaced. This illustrates that hydrogen ions displace bonded hydrogen in the film as efficient as incident carbon ions. This is due to the fact that the momentum transfer from a hydrogen ion to the carbon network is very inefficient in a collision with bonded C atoms but very efficient in a collision with bonded H atoms. As a consequence the kinetic energy of the incident hydrogen ions is largely consumed by hydrogen displacement. Moreover, the influence of the C^+ ion bombardment is expected to be largely compensated by the flux of thermal hydrogen atoms, which can re-saturate any ion-induced defects within their penetration depth of 2 nm (shown as vertical dotted line in Fig. 3).

The ion bombardment mainly alters the distribution of bonded hydrogen in the film in consecutive collision cascades. During such a re-distribution of hydrogen, however, displaced H atoms are able to recombine among each other to form H_2 molecules, which eventually desorb. This process leads to a permanent lowering of the hydrogen content in the films. However, displaced hydrogen might also be able to re-saturate dangling bonds in the film (lattice defects) or at the physical surface (surface dangling bond). The latter process will consume chemisorption sites for incident hydrocarbon radicals. This illustrates that, on one hand, the ion bombardment is able to activate the surface via displacement of surface-bonded hydrogen, but it also causes the formation of sub-surface displaced hydrogen atoms, which can again compensate this surface activation. Preliminary experiments using an 800-eV Ar^+ ion beam and a CH_3 beam show [28], that the rate of the ion-induced surface dangling bond formation is much smaller than expected from the TRIM code due to re-saturation of chemisorption sites by sub-surface displaced hydrogen. A more thorough and quantitative analysis of this effect is at present under investigation.

4. Discussion

Based on the presented results, a schematic picture for the a-C:H growth mechanism is proposed as illustrated in Fig. 4. The growing film surface is separated in a chemistry-dominated growth zone (marked with I in Fig. 4) and an ion-dominated growth zone (marked with II in Fig. 4). This scheme is limited to film deposition from hydrocarbon plasmas with a significant fraction of hydrogen atoms and ions in the growth flux. Therefore, this scheme is suited for most of the standard PECVD processes but not for ion beam deposition of C:H films.

In the chemistry-dominated growth zone, incident atomic hydrogen activates the surface via hydrogen abstraction and creates chemisorption sites for incident saturated hydrocarbon radicals like CH_3. Unsaturated hydrocarbon radicals like C_2H or C_2H_3 have a sticking coefficient of the order of unity and their chemisorption only weakly depends on any surface activation. Furthermore, the H-induced hydrogen elimination reactions lead to a stoichiometry of $H/C \sim 1$ within the penetration range of thermal H in C:H films. This penetration depth is in the range of 2 nm, as has directly been observed

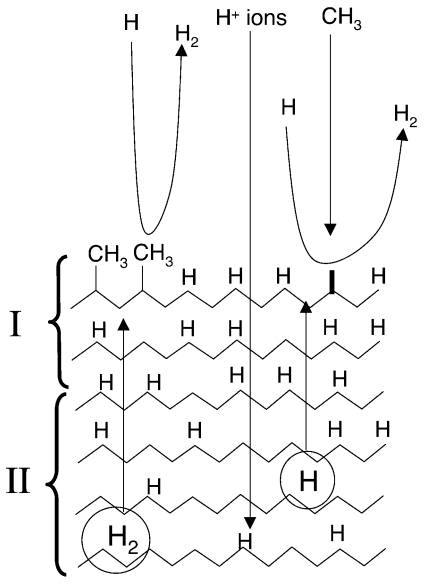

Fig. 4. Schematic of the growing film surface. I: Chemistry dominated growth zone. Incident atomic hydrogen eliminates surface bonded hydrogen via abstraction and creates chemisorption sites for incoming saturated hydrocarbon radicals. II: Ion dominated growth zone. Penetrating ions displace bonded hydrogen within the collision cascade. Displaced hydrogen might recombine to form H_2 molecules or it might re-saturate dangling bonds in the film or at the physical surface.

in plasma experiments [17]. This penetration depth is characteristic for the thickness of the chemistry-dominated growth-zone. It should be mentioned that incident carbon ions have also a penetration depth less than 2 nm at typical ion energies of several 100 eV. Due to the large atomic hydrogen flux towards the growing film surface, however, any ion-induced lowering of the hydrogen content within the carbon ion collision cascade is largely compensated by re-saturation of dangling bonds by thermal H.

In the ion-dominated growth zone, the film structure is altered by displacing hydrogen in a depth beyond the penetration range of thermal H. Especially incident hydrogen ions have a large penetration depth and are very efficient to displace bonded hydrogen in the film. However, most of the displaced hydrogen remains in the film, because any hydrogen diffusion to the surface is negligible at room substrate temperature. Hydrogen atoms in the film are continuously re-distributed in consecutive collision cascades and are able to re-saturate defects in the film and to compensate thereby any the hydrogen- or ion-induced surface activation. They might also recombine and form sub-surface H_2 molecules, which can be trapped in internal voids or desorb form the film. The latter process will lead to decrease of the bulk hydrogen content.

Such a growth mechanism explains the experimental observation that the structure and composition of a-C:H films is often very similar, although different precursor monomers like CH_4, C_2H_6, C_3H_8, C_2H_4 or C_2H_2 are used for plasma-deposition [29,30]. The absence of a monomer retention has been attributed to the fragmentation of monomer molecules in the discharge and to the ion bombardment of the growing film surface. In addition the surface reactions of atomic hydrogen, which is abundant in most hydrocarbon discharges, also largely influence the stoichiometry of a-C:H films. On one hand, incident atomic hydrogen saturates surface dangling bonds or hydrogenates sp^2-coordinated CC surface groups. This leads to an increase of the hydrogen content of a-C:H films. On the other hand, abstraction of surface-bonded hydrogen by incident H creates dangling bonds, which might recombine among each other leading to the formation of new CC bonds. The sequence of hydrogen abstraction and dangling bond recombination lowers the hydrogen content in the film with a stoichiometric limit of $H/C \sim 1$. The important role of atomic hydrogen for film composition is corroborated by the observation that any residual difference in the deposited films from different source gases can be completely eliminated by adding H_2 to the hydrocarbon discharge [30]: an increase of the incident atomic hydrogen flux due to adding H_2 to the source gas shifts the film composition to the stoichiometric limit of $H/C \sim 1$ independent of the H/C ratio of the source gas. The addition of H_2 to the source gas leads also to an increase of the hydrogen content of the films even for varying substrate bias [30].

Any deviation of the film composition from that of films with $H/C \sim 1$ can only be achieved, if (i) the hydrogen content is continuously reduced during growth by an additional energetic ion bombardment or if (ii) the contribution of atomic hydrogen to the growth flux can be minimized. An additional ion bombardment is usually realized by applying a bias at the substrate. The final hydrogen content depends on the rate of hydrogen removal by ion bombardment in comparison to the rate of hydrogen incorporation via adsorption of atomic hydrogen or hydrocarbon radicals. The atomic H flux to the surface can be reduced by using hydrocarbon monomers with a low H/C ratio such as C_2H_2 or C_2H_4. However, the most efficient minimization of the atomic hydrogen flux towards the surface in a hydrocarbon discharge can be achieved by means of a thermal arc plasma from argon with remote acetylene injection [31]. In this type of discharge, the kinetic energy of the incident ions is only a few eV and the ion flux is only a very small fraction of the incident radical flux. By using proper process parameters, an intense and almost pure C_2H radical beam can be produced, which leads to the deposition of hard C:H films with a $H/(H+C)$ ratio of 0.33. Due to the low hydrogen content in the film, a dense layer is formed, which becomes apparent by the significant hardness of the films of ~ 14 GPa.

5. Conclusions

The temperature dependence of a-C:H film formation results from a balance between the temperature-independent incorporation of carbon carrying precursors in competition with the temperature-dependent re-etching of the growing film by atomic hydrogen, which is abundant in any low-temperature plasma from a hydrocarbon precursors gas. The incorporation of carbon-carrying precursors can be characterized by the surface loss probability β. Three characteristic surface loss probabilities can be distinguished: sp^1-hybridized precursors like C_2H have a β of ~ 0.9, sp^2-hybridized precursors have a β of ~ 0.35 and sp^3-hybridized precursors have a $\beta < 10^{-2}$.

The sticking coefficient itself can be measured in a radical-beam experiment, which was performed for the reactants CH_3 and H: CH_3 alone has a sticking coefficient on a a-C:H film surface of only $s(CH_3) \sim 10^{-4}$. This low sticking coefficient, however, can be enhanced by two orders of magnitude to $s(CH_3|H) \sim 10^{-2}$, if an additional flux of atomic hydrogen impinges on to the surface simultaneously. A simple balance equation model of this growth synergism reveals a cross-section for CH_3 chemisorption at a surface-dangling bond between 2.4 and 5.9 $Å^2$.

Incident atomic hydrogen also controls the stoichi-

ometry of the growing film surface. Due to hydrogen elimination reactions, higher hydrides are reduced to mono-hydrides until the final stoichiometry of a polymer-like C:H film of $H/C \sim 1$ is reached. A further reduction of the hydrogen content is only possible by a significant ion bombardment with a penetration depth beyond that of thermal hydrogen. Especially kinetic hydrogen ions are very efficient for the ion-induced removal of bonded hydrogen.

References

[1] H. Tsai, D.B. Bogy, J. Vac. Sci. Technol. A 5 (1987) 3287.
[2] P. Koidl, C. Wild, B. Dischler, J. Wagner, M. Ramsteiner, Mater. Sci. Forum 52/53 (1989) 41.
[3] A.H. Lettington, C. Smith, Diamond Relat. Mater. 1 (1992) 805.
[4] A. Grill, Diamond Relat. Mater. 8 (1999) 428.
[5] W. Möller, Thin Solid Films 228 (1993) 319.
[6] W. Möller, B.M.U. Scherzer, Appl. Phys. Lett. 50 (1870) 1987.
[7] W. Eckstein, Computer Simulation of Ion Solid Interactions, Springer Series in Materials Science, Berlin and Heidelberg, 1991.
[8] Y. Lifshitz, S.R. Kasi, J.W. Rabalais, W. Eckstein, Phys. Rev. B 41 (1990) 10468.
[9] J. Roberston, Diamond Relat. Mater. 2 (1993) 984.
[10] W. Jacob, Thin Solid Films 326 (1998) 1.
[11] P. Pecher, W. Jacob, Appl. Phys. Lett. 73 (1998) 31.
[12] H. Toyoda, H. Kojima, H. Sugai, Appl. Phys. Lett. 54 (1989) 1507.
[13] M. Shiratani, J. Jolly, H. Videlot, J. Perrin, Jap. J. Appl. Phys. 36 (1997) 4752.
[14] J. Perrin, M. Shiratani, P. Kae-Nune, H. Videlot, J. Jolly, J. Guillon, J. Vac. Sci. Technol. A 16 (1998) 278.
[15] C. Hopf, K. Letourneur, W. Jacob, T. Schwarz-Selinger, A. von Keudell, Appl. Phys. Lett. 74 (1999) 3800.
[16] C. Hopf, T. Schwarz-Selinger, W. Jacob, A. von Keudell, J. Appl. Phys. 87 (2000) 2719.
[17] A. von Keudell, W. Jacob, J. Appl. Phys. 79 (1996) 1092.
[18] T. Schwarz-Selinger, A. von Keudell, W. Jacob, J. Vac. Sci. Technol. A. 18 (2000) 995.
[19] T. Schwarz-Selinger, V. Dose, W. Jacob, A. von Keudell, J. Vac. Sci. Technol. A. 19 (2001) 101.
[20] A. von Keudell, T. Schwarz-Selinger, M. Meier, W. Jacob, Appl. Phys. Lett. 76 (2000) 676.
[21] A. von Keudell, T. Schwarz-Selinger, W. Jacob, J. Appl. Phys. 89 (2001) 2979.
[22] J. Küppers, Surf. Sci. Rep. 22 (1995) 249.
[23] M. Meier, A. von Keudell, J. Appl. Phys. 90 (2001) 3585.
[24] A. von Keudell, Thin Solid Films 402 (2002) 1.
[25] J.C. Angus, F. Jansen, J. Vac. Sci. Technol. A 6 (1988) 1778.
[26] J. Robertson, Phys. Rev. Lett. 68 (1992) 220.
[27] A. von Keudell, W. Möller, R. Hytry, Appl. Phys. Lett. 62 (1993) 937.
[28] C. Hopf, A. von Keudell (unpublished).
[29] P. Koidl, C. Wild, R. Locher, R.E. Sah, in: R.E. Clausing, L.L. Horton, J.C. Angus, P. Koidl (Eds.), Diamond and Diamond-like Films and Coatings, NATO-ASI Series B: Physics, vol. 266, Plenum, New York, 1991, pp. 155–158.
[30] T. Schwarz-Selinger, A. von Keudell, W. Jacob, J. Appl. Phys. 86 (7) (1999) 3988.
[31] J.W.A.M. Gielen, M.C.M. van de Sanden, D. Schram, Appl. Phys. Lett. 69 (1996) 152.